J|A|C|S ARTICLES

Published on Web 10/30/2009

Dynamics of Photochemical Electron Injection and Efficiency of Electron Transport in DNA

Pierre Daublain,[†] Arun K. Thazhathveetil,[†] Qiang Wang,[‡] Anton Trifonov,[‡] Torsten Fiebig,*[,‡] and Frederick D. Lewis*[,†]

Departments of Chemistry, Northwestern University, Evanston, Illinois 60208-3113, and Boston College, Chestnut Hill, Massachusetts 02467

Received June 22, 2009; E-mail: fdl@northwestern.edu; fiebig@bc.edu

Abstract: The dynamics of electron injection and quantum yields for photoinduced dehalogenation have been investigated in a series of DNA hairpins possessing an aminopyrene capping group. Aminopyrene serves as an electron donor and is separated from a bromo- or iodoracil electron trap by 1 to 7 A-T base pairs. Broad band femtosecond transient absorption spectra and fluorescence quantum yield measurements are indicative of rapid and efficient charge separation. The resulting charge-separated state decays predominantly via charge recombination on the picosecond time scale. Steady-state irradiation in the presence of 0.1 M *i*-PrOH results in loss of halogen and conversion of the halouracil-containing conjugates to the corresponding uracil-containing conjugates in high yield. Dehalogenation occurs via a multistep mechanisms consisting of electron injection, electron transport to the halouracil, loss of halide, and trapping of the uracilyl radical. Quantum yields for product formation decrease by a factor of 2 for each additional A-T base pair interposed between the aminopyrene and bromouracil. This distance dependence is similar to that observed in our studies of DNA hole transport in stilbene donor−acceptor capped hairpins; however, the quantum yields for product formation are much lower for the aminopyrene conjugates as a consequence of more rapid charge recombination.

Introduction

Charge transport in DNA can occur by either movement of positive charge (holes) or negative charge (electrons) between the π-stacked bases which constitute the hydrophobic core of duplex DNA.[1] Experimental studies of photoinduced hole transport have employed various methods for the oxidation of the purine bases adenine and guanine (A and G), which have lower oxidation potentials than the pyrimidines thymine, cytosine, and uracil (T, C, and U), whereas studies of electron transport have employed several methods for the reduction of pyrimidines, which have lower reduction potentials than the purines.[2] Chemical evidence for hole transport across multiple base pairs has been provided by strand cleavage or ring-opening isomerization at hole-trapping sites (e.g., multiple guanines, deazagunaine, or *N*-cyclopropyladenine).[3] Initial evidence for electron transport across multiple base pairs was provided by studies of reductive cleavage of thymine dimers ($T<>T$)[4−6] using reduced flavins as the electron donor.[7] These studies established that electron transport is weakly dependent upon the intervening base sequence. Reductive cleavage of a thymine oxetane[8] and loss of halide ion from reduced 5-bromouracil and iodoracil have also been used as chemical probes of electron transport.[9−13] Transient absorption spectroscopy has been used to detect the radical ion intermediates and to determine quantum yields and dynamics for hole transport.[14−16] Considerably less is known about the dynamics and efficiency of electron transport in DNA.

The initial studies of electron injection and migration using ionizing radiation (radiolysis) as the source of electrons were reported a half-century ago.[17] Subsequent studies of electron transport following attachment of solvated electrons to duplex DNA established that electrons could migrate over distances up to 10−12 base pairs at room temperature and longer distances at low

[†] Northwestern University.
[‡] Boston College.

(1) (a) Lewis, F. D. In *Electron Transfer in Chemistry*; Balzani, V., Ed.; Wiley-VCH: Weinheim, Germany, 2001; Vol. 3, pp 105−175. (b) Schuster, G. B., Ed.; *Long-Range Charge Transfer in DNA, I and II*; Springer: New York, 2004; Vol. 236, p 237. (c) Wagenknecht, H. A. *Charge Transfer in DNA*; Wiley-VCH: Weinheim, 2005.
(2) Seidel, C. A. M.; Schulz, A.; Sauer, M. H. M. *J. Phys. Chem.* **1996**, *100*, 5541–5553.
(3) (a) Schuster, G. B. *Acc. Chem. Res.* **2000**, *33*, 253–260. (b) Giese, B. *Acc. Chem. Res.* **2000**, *33*, 631–636. (c) Holmlin, R. E.; Dandliker, P. J.; Barton, J. K. *Angew. Chem., Int. Ed. Engl.* **1997**, *36*, 2714–2730. (d) Nakatani, K.; Dohno, C.; Saito, I. *J. Am. Chem. Soc.* **1999**, *121*, 10854–10855. (e) Nakatani, K.; Dohno, C.; Saito, I. *J. Am. Chem. Soc.* **2001**, *123*, 9681–9682. (f) Dohno, C.; Ogawa, A.; Nakatani, K.; Saito, I. *J. Am. Chem. Soc.* **2003**, *125*, 10154–10155. (g) Dohno, C.; Stemp, E. D. A.; Barton, J. K. *J. Am. Chem. Soc.* **2003**, *125*, 9586–9587. (h) Elias, B.; Genereux, J. C.; Barton, J. K. *Angew. Chem., Int. Ed.* **2008**, *47*, 9067–9070.
(4) (a) Schwögler, A.; Burgdorf, L. T.; Carell, T. *Angew. Chem., Int. Ed.* **2000**, *39*, 3918–3920. (b) Breeger, S.; Hennecke, U.; Carell, T. *J. Am. Chem. Soc.* **2004**, *126*, 1302–1303. (c) Giese, B.; Carl, B.; Carl, T.; Carell, T.; Behrens, C.; Hennecke, U.; Schiemann, O.; Feresin, E. *Angew. Chem., Int. Ed.* **2004**, *43*, 1848–1851.
(5) Behrens, C.; Burgdorf, L. T.; Schwogler, A.; Carell, T. *Angew. Chem., Int. Ed.* **2002**, *41*, 1763–1766.
(6) Haas, C.; Kraling, K.; Cichon, M.; Rahe, N.; Carell, T. *Angew. Chem., Int. Ed.* **2004**, *43*, 1842–1844.
(7) Behrens, C.; Cichon, M. K.; Grolle, F.; Hennecke, U.; Carell, T. *Top. Cur. Chem.* **2004**, *236*, 187–204.
(8) Stafforst, T.; Diederichsen, U. *Angew. Chem., Int. Ed.* **2006**, *45*, 5376–5380.

 10.1021/ja905140n CCC: $40.75

temperatures, prior to capture by electron scavengers including 5-bromo- and 5-iodoracil (^{Br}U and ^{I}U) and methylviologen.[18−20] A recent pulse radiolysis study of electron transfer from reduced naphthalimide to ^{I}U by Kawai et al. demonstrated that 3 or 4 A:T base pairs are sufficient to inhibit electron transfer at room temperature in this system.[21] This result was interpreted as evidence for much lower mobility for electron transport than observed by these workers for hole transport in A-tracts.[22]

Studies of the dynamics and efficiency of photoinduced electron injection in duplex DNA conjugates have been few in number. Lewis and Wasielewski investigated the dynamics of electron injection in synthetic hairpins having a stilbenediether linker and several different adjacent base pairs.[23] Ultrafast electron injection ($\tau_i < 0.5$ ps) and charge recombination ($\tau_{cr} \approx$ 20 ps) were observed for adjacent A:T or A:^{Br}U base pairs and somewhat slower injection and recombination for an adjacent G:C base pair. Wagenknecht and Fiebig[24] investigated the dynamics of electron injection in duplexes possessing a pyrene-modified uracil as the electron donor and halouracils as the electron traps. They observed rapid (2−3 ps) formation of the $Py^{+\bullet}$-$U^{-\bullet}$ charge-separated state and complex charge recombination dynamics, attributed to multiple duplex conformations.[24] They also investigated strand cleavage resulting from loss of bromide from ^{Br}U and found that the presence of a single A:T base pair between Py-U and ^{Br}U significantly reduced the relative strand cleavage yield. In contrast, Barton and co-workers report a shallow distance dependence for the relative yields of products resulting from loss of bromide from reduced ^{Br}U generated using a flash-quench technique which produces a ground state reductant capable of reducing both T and ^{Br}U.[13]

Theoretical studies of electron transport in DNA have also been more limited in scope and number than studies of hole transport.[25] Bixon et al. suggested that electron transport in random base sequences should be more favorable than hole transport due to the similar reduction potentials of T and C.[26] Voityuk et al. used semiempirical methods to calculate the electron affinities of several base triads and noted the absence of a triad composed of common bases that could serve as an electron trap.[27] Calculated gas phase electron affinities for the nucleobases ^{Br}U and T indicate that the former is larger by ca. 0.5 eV;[28] however, solution oxidation potentials were not available for the halouracils prior to initiation of the present study.

We report here the results of a collaborative investigation of the dynamics and photochemical consequences of electron injection in a family of DNA hairpins possessing a 5′-tethered aminopyrene derivative (APy, Chart 1a) designed to function as a hairpin capping group and a single ^{X}U:A base pair (X = bromine or iodine, Chart 1b)) separated from the aminopyrene by 0 to 7 A-T base pairs (Chart 1c). Pyrene derivatives have been widely investigated in studies of DNA electron transfer and can serve as electron donors and acceptors, depending upon the choice of substituent.[19,24,29−31] However, information about

Chart 1. Structures of (a) **APy-H** and the **APy** Capping Group, (b) Pyrimidines, and (c) **APy-n^{Br}U** Conjugates

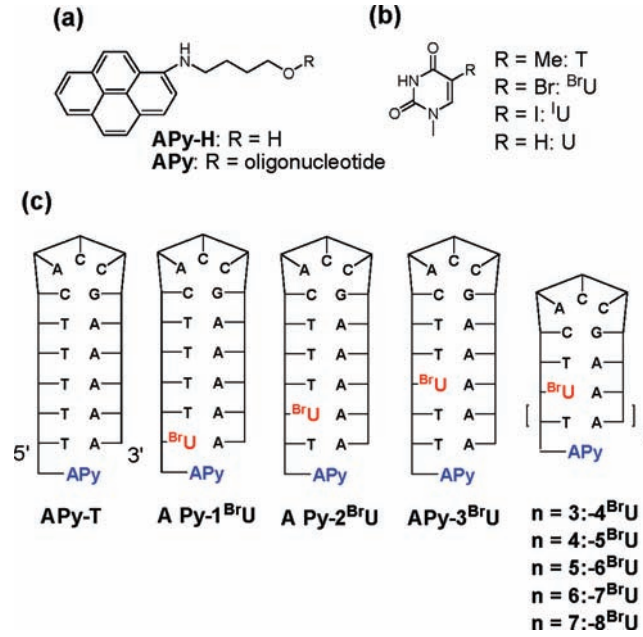

(9) Ito, T.; Hayashi, A.; Kondo, A.; Uchida, T.; Tanabe, K.; Yamada, H.; Nishimoto, S. *Org. Lett.* **2009**, *11*, 927–930.
(10) Ito, T.; Rokita, S. E. *J. Am. Chem. Soc.* **2003**, *125*, 11480–11481.
(11) Ito, T.; Rokita, S. E. *J. Am. Chem. Soc.* **2004**, *126*, 15552–15559.
(12) Manetto, A.; Breeger, S.; Chatgilialoglu, C.; Carell, T. *Angew. Chem., Int. Ed.* **2006**, *45*, 318–321.
(13) Elias, B.; Shao, F. W.; Barton, J. K. *J. Am. Chem. Soc.* **2008**, *130*, 1152–1153.
(14) (a) von Feilitzsch, T.; Tuma, J.; Neubauer, H.; Verdier, L.; Haselsberger, R.; Feick, R.; Gurzadyan, G.; Voityuk, A. A.; Griesinger, C.; Michel-Beyerle, M. E. *J. Phys. Chem. B* **2008**, *112*, 973–989. (b) Kawai, K.; Osakada, Y.; Fujitsuka, M.; Majima, T. *Chem.—Eur. J.* **2008**, *14*, 3721–3726.
(15) Lewis, F. D.; Zhu, H.; Daublain, P.; Fiebig, T.; Raytchev, M.; Wang, Q.; Shafirovich, V. *J. Am. Chem. Soc.* **2006**, *128*, 791–800.
(16) Vura-Weis, J.; Wasielewski, M. R.; Thazhathveetil, A. K.; Lewis, F. D. *J. Am. Chem. Soc.* **2009**, *131*, 9722–9727.
(17) Steenken, S. *Chem. Rev.* **1989**, *89*, 503–520. Becker, D.; Sevilla, M. D. *Adv. Radiation Biol.* **1993**, *17*, 121–180.
(18) Yan, M.; Becker, D.; Summmerfield, S.; Renke, P.; Sevilla, M. D. *J. Phys. Chem.* **1992**, *96*, 1983–1989.
(19) Shafirovich, V. Y.; Dourandin, A.; Luneva, N. P.; Geacintov, N. E. *J. Phys. Chem. B.* **1997**, *101*, 5863–5868.
(20) Messer, A.; Carpenter, K.; Forzley, K.; Buchanan, J.; Yang, S.; Razskazovskii, Y.; Cai, Y. L.; Sevilla, M. D. *J. Phys. Chem. B* **2000**, *104*, 1128–1136.
(21) Kawai, K.; Kimura, T.; Kawabata, K.; Tojo, S.; Majima, T. *J. Phys. Chem. B.* **2003**, *107*, 12838–12841.
(22) Kawai, K.; Takada, T.; Tojo, S.; Fujitsuka, M.; Majima, T. *J. Am. Chem. Soc.* **2003**, *125*, 6842–6843.
(23) Lewis, F. D.; Liu, X.; Miller, S. E.; Hayes, R. T.; Wasielewski, M. R. *J. Am. Chem. Soc.* **2002**, *124*, 11280–11281.
(24) Kaden, P.; Mayer-Enthart, E.; Trifonov, A.; Fiebig, T.; Wagenknecht, H.-A. *Angew. Chem., Int. Ed.* **2005**, *44*, 1636–1639.
(25) (a) Berlin, Y. A.; Beratan, D.; Kurnikov, I. V.; Ratner, M. A.; Burin, A. L. *Top. Cur. Chem.* **2004**, *237*, 1–36. (b) Schuster, G. B.; Landman, U. *Top. Cur. Chem.* **2004**, *236*, 139–161. (c) Conwell, E. M.; Bloch, S. M.; McLaughlin, P. M.; Basko, D. M. *J. Am. Chem. Soc.* **2007**, *129*, 9175–9181.
(26) Bixon, M.; Giese, B.; Wessely, S.; Langenbacher, T.; Michel-Beyerle, M. E.; Jortner, J. *Proc. Natl. Acad. Sci. U.S.A.* **1999**, *96*, 11713–11716.
(27) Voityuk, A. A.; Michel-Beyerle, M. E.; Rösch, N. *Chem. Phys. Lett.* **2001**, *342*, 231–238.
(28) Li, X. F.; Sevilla, M. D.; Sanche, L. *J. Am. Chem. Soc.* **2003**, *125*, 8916–8920.
(29) Manoharan, M.; Tivel, K. L.; Zhao, M.; Nafisi, K.; Netzel, T. L. *J. Phys. Chem.* **1995**, *99*, 17461–17472. (b) Telser, J.; Cruickshank, K. A.; Morrison, L. E.; Netzel, T. L.; Chan, C. K *J. Am. Chem. Soc.* **1989**, *111*, 7226–7232. (c) Geacintov, N. E.; Solntsev, K.; Johnson, L. W.; Chen, J. X.; Kolbanovskiy, A. D.; Liu, T. M.; Shafirovich, V. Y. *J. Phys. Org. Chem.* **1998**, *11*, 561–565. (d) Zahavy, E.; Fox, M. A. *J. Phys. Chem. B* **1999**, *103*, 9321–9327. (e) Shafirovich, V. Y.; Courtney, S. H.; Ya, N.; Geacintov, N. E. *J. Am. Chem. Soc.* **1995**, *117*, 4920–4929. (f) Shafirovich, V. Y.; Geacintov, N. E. *Top. Cur. Chem.* **2004**, *237*, 129–157. (g) Shafirovich, V. Y.; Levin, P. P.; Kuzmin, V. A.; Thorgeirsson, T. E.; Kliger, D. S.; Geacintov, N. E. *J. Am. Chem. Soc.* **1994**, *116*, 63–72.

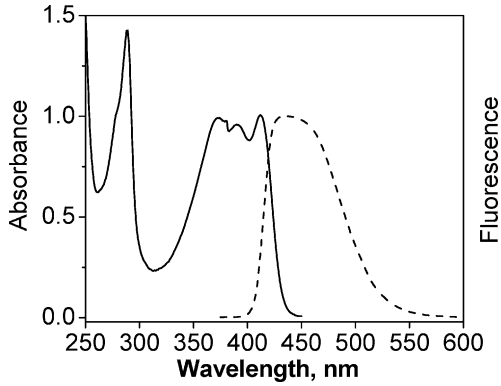

Figure 1. UV (solid line) and fluorescence spectra (dashed line) of **APy-H** in methanol.

the dynamics of electron injection and resulting products is available only in the previously mentioned study of a pyrene-modified uracil.[24] Netzel et al. attributed weak fluorescence from a covalently linked pyrenyluridine to fast charge recombination in the CT state.[30] A recent claim of RNA-mediated electron transfer from pyrene to nitrobenzene relies exclusively on pyrene fluorescence quantum yields to assess the distance dependence.[32] On the basis of its singlet energy and oxidation potential, singlet 1-aminopyrene was expected to serve as a strong electron donor (like the aminoarenes investigated by Ito and Rokita[10,11]), capable of reducing pyrimidine bases but not oxidizing purine bases. The dynamics of photoinduced electron injection were determined by means of femtosecond broadband transient absorption spectroscopy. Quantum yields for loss of halogen from ^{X}U were determined by HPLC and MALDI-TOF analysis of irradiated solutions containing isopropyl alcohol as a free radical scavenger for the uracilyl radical. Quantum yields decrease by ca. a factor of 2 for each additional intervening A-T base pair, resulting in a linear dependence of ln(Φ) upon the distance between APy and ^{X}U. This distance dependence is compared to reported values for other electron transport systems and with our results for hole transport in capped hairpins possessing polyA:polyT base pair domains.[16,33]

Results

Absorption and Fluorescence Spectra of the Aminopyrene Derivatives. The UV absorption and fluorescence spectra of *N*-(4-hydroxybutyl)-1-aminopyrene (**APy-H**, Chart 1a) in methanol are shown in Figure 1. The absorption bands are red-shifted and broadened with respect to those of pyrene, as is the case for other aromatic amines.[34] Further information about the UV absorption spectrum was obtained using semiempirical ZINDO calculations for the reference molecule *N*-methyl-1-aminopyrene. The long-wavelength absorption band is assigned to overlapping $\pi-\pi^*$ transitions with maxima at 371 and 345 nm and log(ε) = 3.7 and 4.7, respectively, both of which have aminopyrene→ pyrene character (Figure S1, Supporting Information). **APy-H** has a fluorescence quantum yield $\Phi_{fl} = 0.67$ and lifetime $\tau_S =$ 6.2 ns, similar to the values reported for 1-aminopyrene in methanol or water.[35]

The APy conjugates (Chart 1b) were prepared using methods previously employed for stilbene-capped hairpin conjugates.[36] The UV absorption and the fluorescence spectra of the conjugate **APy-T** in aqueous buffer are shown in Figure S2 (Supporting Information). Its absorption spectrum is broadened and red-shifted by several nm, when compared to the spectrum of **APy-H** in methanol (Figure 1). All of the **APy-n^{Br}U** and **APy-n^{I}U** conjugates are very weakly fluorescent ($\Phi_{fl} < 0.005$) and thus their fluorescence decay times were not measured. Protonation of the amine group in **APy-T** results in replacement of the long-wavelength absorption band with a structured band at shorter wavelength. Protonation in acetate buffer solution is observed at pH = 4.0, but not at pH > 5.0, consistent with the pK_a value of 4.6 for anilinium.[37]

Conjugates **APy-T** and **APy-3^{Br}U** have melting temperatures of $T_m = 62.9$ and 64.5 °C, respectively, as determined from the derivatives of their 260 nm thermal dissociation profiles (Figure S3, Supporting Information). The circular dichroism spectra of the APy conjugates (Figure S4, Supporting Information) display very weak bands at wavelengths longer than 300 nm, attributed to induced CD of the APy chromophore,[38] and stronger bands between 200−300 nm, similar to those for the duplex poly(dA):poly(dT).[39]

Pump−Probe Spectra. Transient spectra for **APy-H** obtained using a pump wavelength of 415 nm are shown in Figure 2a. These spectra display a relatively narrow negative band at 420 nm and a broad absorption band at longer wavelengths, which are formed during the pump pulse (ca. 100 fs). The 420 band and a long-wavelength shoulder decay within several ps leaving a structured negative band at 420 nm assigned to the ground state bleach and positive bands at 320 and 510 nm assigned to the absorption of aminopyrene ^{1}S*. Global analysis of the transient spectra provide spectra associated with the short-and long-lived species (Figure S5a, Supporting Information). The short-lived species displays negative bands at 420 and 460 nm assigned to stimulated emission of ^{2}S* and a positive band at 520 nm assigned to ^{2}S* absorption. The long-lived species has a negative band at 440 nm assigned to the ground state bleach and positive bands at 320 and 500 nm assigned to ^{1}S* absorption. These bands decay slowly on the 1.9 ns time scale of the transient measurements, in accord with the observed fluorescence decay time.

The transient spectra of **APy-T** are shown in Figure 2b. The 430 and 530 nm bands are formed during the pump pulse and decay within the first few ps, leaving a negative band at 400 nm and a positive bands at 310 and 480 nm. Global analysis of the transient spectra provides three components whose associated spectra are shown in Figure S5b, Supporting Information. The

(30) Gaballah, S. T.; Collier, G.; Netzel, T. L. *J. Phys. Chem. B* **2005**, *109*, 12175–12181.
(31) Gaballah, S. T.; Vaught, J. D.; Eaton, B. E.; Netzel, T. L. *J. Phys. Chem. B* **2005**, *109*, 5927–5934.
(32) Maie, K.; Miyagi, K.; Takada, T.; Nakamura, M.; Yamana, K. *J. Am. Chem. Soc.* **2009**, *131*, 13188–13189.
(33) Lewis, F. D.; Daublain, P.; Cohen, B.; Vura-Weis, J.; Shafirovich, V.; Wasielewski, M. R. *J. Am. Chem. Soc.* **2007**, *129*, 15130–15131.
(34) (a) Ruckert, I.; Demeter, A.; Morawski, O.; Kuhnle, W.; Tauer, E.; Zachariasse, K. A. *J. Phys. Chem. A* **1999**, *103*, 1958–1966. (b) Lewis, F. D.; Hougland, J. L.; Markarian, S. A. *J. Phys. Chem. A* **2000**, *104*, 3261–3268.
(35) Sarpal, R. S.; Dogra, S. K. *J. Chem. Soc., Faraday Trans.* **1992**, *88*, 2725–2731.
(36) Zhang, L.; Zhu, H.; Sajimon, M. C.; Stutz, J. A. R.; Siegmund, K.; Richert, C.; Shafirovich, V.; Lewis, F. D. *J. Chinese Chem. Soc. (Taipei)* **2006**, *53*, 1501–1507.
(37) Isaacs, N. S. *Physical Organic Chemistry*, 2nd ed.; Longman: Essex, England, 1995.
(38) Ardhammar, M.; Kurucsev, T. ; Nordén, B. In *Circular Dichroism, Principles and Applications*; Berova, N., Nakanishi, K., Woody, R. W., Eds.; Wiley-VCH: New York, 2000; pp 741−768.
(39) Johnson, W. C. In *Circular Dichroism, Principles and Applications*; Berova, N., Nakanishi, K., Woody, R. W., Eds.; Wiley-VCH: New York, 2000; pp 703−718.

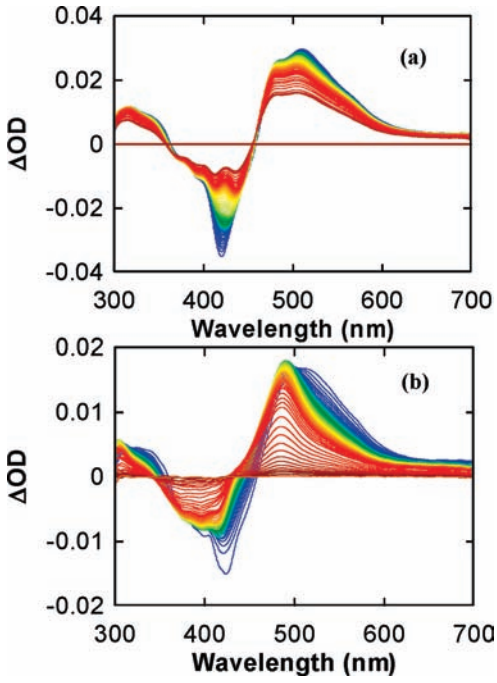

Figure 2. Transient absorption spectra for (a) **APy-H** in methanol at delay times of 0−1.0 ns and (b) **APy-T** in aqueous buffer at delay times of 0−100 ps. Color code: blue 0−1.0 ps, green-yellow 1−5 ps, red >5 ps.

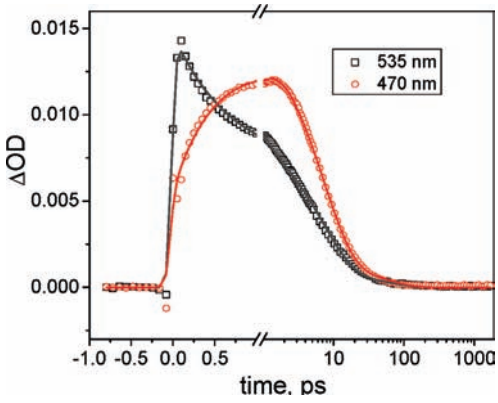

Figure 3. Single wavelength transient kinetic traces for **APy-T** and fits obtained from global analysis of the 470 and 535 nm transients.

0.55 ps component is similar in band shape to the short-lived component of **APy-H** and is assigned to ^{2}S* stimulated emission and absorption. The 7.1 and 32 ps components both have spectral band shapes similar to that reported the cation radical **APy**$^{+\bullet}$[40] and are assigned to APy$^{+\bullet}$-T$^{-\bullet}$ charge-separated states.

Global fitting of the 470 and 535 nm transients of **APy-T** provides a rise time attributed to formation of the charge-separated state and two decay times attributed to charge recombination (Figure 3). The rise and decay times for **APy-1^{Br}U** and **APy-2^{Br}U** are somewhat shorter than those for **APy-T**, **APy-3^{Br}U**, and **APy-4^{Br}U** which have similar kinetic parameters (Table 1). The absence of a long-lived transient associated with formation of solvated electrons, is consistent with electron injection into a neighboring base pair rather than into water, a process which has been reported to occur upon laser excitation of pyrene derivatives in water.[19]

Table 1. Transient Kinetics for the **APy** Conjugates[a]

conjugate[b]	τ_{cs}, ps[c]	τ_{cr}, ps[d]
APy-T	0.55(−64)	7.1(92), 52(8)
APy-1^{Br}U	0.27(−67)	2.4(96), 57(4)
APy-2^{Br}U	0.29(−61)	4.4(87), 43(13)
APy-3^{Br}U	0.53(−66)	6.5(89), 57(11)
APy-4^{Br}U	0.54(−67)	6.9(92), 66(8)

[a] Data for pulsed laser excitation at 415 nm. Kinetic data are obtained from global fitting of 470 and 535 nm kinetic traces and preexponentials (in parentheses) are obtained from 470 nm data. Similar decay times are obtained from the single wavelength 480 ns decays and recovery of the ground state bleach at 400 nm. [b] See Chart 1b for structures. [c] Component attributed to charge separation. [d] Components attributed to charge recombination.

Photochemistry of the APy Conjugates. Dilute solutions of the APy conjugates containing 0.1 M NaCl and 0.1 M *i*-PrOH were deoxygenated and irradiated on an optical bench with monochromatic 390 nm light corresponding to the aminopyrene absorption maximum. The use of *i*-PrOH as an efficient scavenger for the uracilyl radical has been described by Sugiyama and Saito.[41,42] Aliquots were removed and analyzed periodically either directly by HPLC with UV diode array detection or by MALDI-TOF mass spectrometry of samples collected by HPLC.

APy-T is stable under our irradiation conditions. A major product peak corresponding to loss of bromide or iodide and formation of uracil-containing conjugates was observed for all of the ^{Br}U-containing conjugates except **APy-1^{Br}U**.[43] Loss of bromide or iodide was confirmed by mass spectrometry of the product peaks collected by HPLC and, in selected cases, by comparison of HPLC and mass spectral data with that for authentic samples of the **APy-nU** conjugates possessing uracil in place of ^{Br}U or ^{I}U (Table S1, Supporting Information). HPLC data for conversion of **APy-4^{Br}U** and **APy-4^{I}U** to **APy-4U** for different irradiation times are shown in Figure S6 (Supporting Information). The HPLC data shows better separation of reactant and product peaks for **APy-4^{I}U** vs **APy-4^{Br}U** and the formation of a minor product for **APy-4^{Br}U** (accounting for ca. 5% of the total product) but not for **APy-4^{I}U**. The mass balance for product formation is ca. 90% at 50% conversion of reactants and decreases slightly at higher conversions which require longer irradiation times (Figure S7, Supporting Information). The separation of reactant and product peaks by HPLC under nondenaturing conditions decreases as the distance between the pyrene capping group and ^{X}U increases, necessitating the use of quantitative MALDI analysis[44] for the **APy-6−8^{Br}U** conjugates. HPLC and MALDI analysis for serveral of closely related conjugates provided similar results, providing confidence in the MALDI data.

Plots of conversion vs irradiation time for the **APy-n^{Br}U** and **-n^{I}U** conjugates are shown in Figures 4 and S8, respectively. These plots show downward curvature at conversions above 50% (Figure S7, Supporting Information), as a consequence of depletion of reactant. Relative quantum yields for the formation

(40) Oyama, M.; Higuchi, T.; Okazaki, S. *Electrochem. Commun.* **2001**, *3*, 363–366.
(41) Sugiyama, H.; Tsutsumi, Y.; Saito, I. *J. Am. Chem. Soc.* **1990**, *112*, 6720–6721.
(42) Fujimoto, K.; Sugiyama, H.; Saito, I. *Tetrahedron Lett.* **1998**, *39*, 2137–2140.
(43) In the case of **APy-1^{Br}U**, two product peaks were detected by HPLC, both of which have molecular weights corresponding to loss of bromide. We did not attempt to identify these products or measure the quantum yields for their formation.
(44) Bruenner, B. A.; Yip, T. T.; Hutchens, T. W. *Rapid Commun. Mass Spectrom.* **1996**, *10*, 1797–1801.

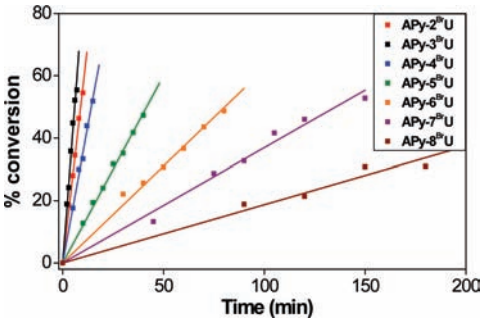

Figure 4. Time evolution of the formation **APy-nU** upon 390 nm irradiation of **APy-n^{Br}U** conjugates in aqueous buffer containing 0.1 M *i*-PrOH. Data for **APy-1**−**5^{Br}U** obtained from HPLC analysis and for **APy-6**−**8^{Br}U** from MALDI analysis of irradiated solutions.

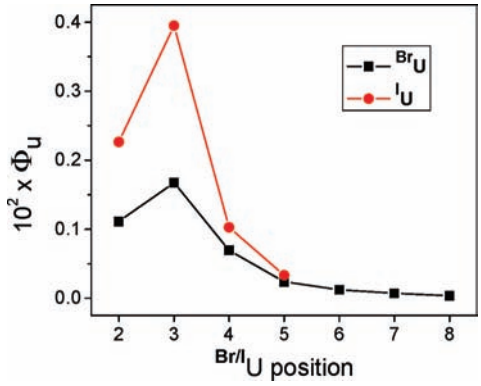

Figure 5. Dependence of the quantum yield formation of **APy-nU** from **APy-n^{Br}U** and **Py-n^{I}U** upon the location of the halouracil.

of the **APy-nU** conjugates were determined from the initial slopes of these plots. Absolute quantum yields (Φ_U) were determined for **APy-4^{Br}U** using monochromatic irradiation of the pyrene chromophore and potassium ferrioxalate chemical actinometry (see Experimental Section).[45] The resulting quantum yields are shown in Figure 5. The absolute values of Φ_U are small, however our analytical methods permit determination of Φ_U with a good level of precision.

Electrochemical Measurements. The oxidation potential of **APy-H** in dimethyl formamide (DMF) containing 0.1 M tetra-*n*-butylammonium hexafluorophosphate determined by means of cyclic voltammetry using ferrocene/ferrocinium as an internal reference ($FeCp_2^{0/+}$ = 0.47) is 0.60 ± 0.05 V vs SCE.[46] Reduction potentials determined by square wave voltammetry for the pyrimidine deoxynucleosides T, C, U, ^{Br}U, and ^{I}U are −2.35, −2.48, −2.30, −1,86, and −1.82 ± 0.05 V vs SCE, respectively. Our values for T, C, and U are similar to those reported by Seidel, et al.[2] when corrected for the difference in reference electrode potentials (SCE vs NHE).

Discussion

Electron Injection. The linked aminopyrene **APy-H** (Chart 1a) was selected for this study of DNA electron injection on the basis of its ease of incorporation into DNA hairpin structures, spectroscopic properties (Figure 1), and low oxidation potential (see below). The APy conjugates possess a single GC base pair adjacent to an ACC loop, a base sequence known to promote the formation of stable mini-hairpins.[47] Capped hairpins offer the advantage of forming stable base-paired structures whose thermal stability is independent of concentration. Replacement of one thymine base in the **APy-T** capped hairpin with ^{Br}U results in a modest increase in thermal stability (Figure S3, Supporting Information), as previously reported for DNA duplexes containing ^{Br}U.[48]

Pyrene derivatives are known to serve as either electron donors for the reduction of pyrimidine bases or electron acceptors for the oxidation of purine bases.[24,30,31] The energetics of photoinduced electron injection from singlet APy to a neighboring pyrimidine can be approximated using Weller's equation (eq 1),

$$\Delta G_{et} = -E_s - (E_{rdn} - E_{ox}) + (2.6/\varepsilon - 0.13\text{eV}) \quad (1)$$

where E_s is the singlet energy of **APy-H** (2.84 eV), E_{ox} is its oxidation potential (0.60 V vs SCE in DMF), E_{rdn} is the reduction potential of the neighboring pyrimidine base, and final term is an empirical correction for the solvent-dependent Coulomb attraction energy (−0.06 eV in DMF).[49] Using the reduction potentials determined in this study for the pyrimidine nucleosides in DMF, the calculated values of ΔG_{et} for photoreduction of T, ^{Br}U, and ^{I}U are +0.05, −0.64, and −0.68 V, respectively. We note that the potentials for both **APy-H** and the pyrimidines are likely to be different within the base-paired hairpin structure in water than for the isolated molecules in DMF. Thus the values of ΔG_{et} calculated using eq 1 are at best rough approximations.

The fs transient absorption spectra of **APy-H** (Figure 2a) display the rapid decay of transient bands assigned to pyrene ^{2}S* with formation of a long-lived transient assigned to pyrene ^{1}S*. ^{2}S*→^{1}S* internal conversion has been reported to occur on the subps time scale for pyrene and several of its derivatives.[50,51] The somewhat longer decay time of **APy-H** in methanol may be related to delocalization of the aminopyrene singlet states (Figure S1, Supporting Information) or hydrogen bonding of the secondary amine with solvent.[34] The transient absorption spectra of **APy-T** (Figure 2b) display similar ^{2}S* decay on the subps time scale with formation of an absorption band which is narrower and blue-shifted when compared to the spectrum of **APy-H**. This **APy-T** band is similar, both in band shape and wavelength, to spectra reported for the cation radical of aminopyrene (generated either by electron transfer using the tris(*p*-bromophenyl)-amine cation radical[40] or photoinduced charge separation in a urea-linked aminopyrene-nitrobenzene dyad[51]). Thus we conclude that excitation of **APy-T** results in fast and efficient formation of the $APy^{+\bullet}T^{-\bullet}$ charge-separated state. Fast charge separation is consistent with the low values of Φ_{fl} observed for **APy-T** and is indicative of exergonic electron transfer quenching, rather than the slightly endergonic value of ΔG_{et} obtained using single nucleotide potentials and

(45) Murov, S. L. *Handbook of Photochemistry*; Marcel Dekker: New York, 1973.
(46) Astruc, D. In *Electron Transfer in Chemistry*; Balzani, V., Ed.; Wiley-VCH: Weinheim, 2001; Vol. 2, pp 714−803.
(47) (a) Yoshizawa, S.; Kawai, G.; Watanabe, K.; Miura, K.; Hirao, I. *Biochemistry* **1997**, *36*, 4761–4767. (b) Lewis, F. D.; Zhang, L.; Liu, X.; Zuo, X.; Tiede, D. M.; Long, H.; Schatz, G. S. *J. Am. Chem. Soc.* **2005**, *127*, 14445–14453.
(48) Becher, G.; He, J. L.; Seela, F. *Helv. Chim. Acta* **2001**, *84*, 1048–1065.
(49) Weller, A. *Zeit. Phys. Chem. Neue. Folg.* **1982**, *133*, 93–98.
(50) Raytchev, M.; Pandurski, E.; Buchvarov, I.; Modrakowski, C.; Fiebig, T. *J. Phys. Chem. A* **2003**, *107*, 4592–4600.
(51) Lewis, F. D.; Daublain, P.; Delos Santos, G.; Liu, W.; Asatryan, A. M.; Markarian, S. A.; Fiebig, T.; Raytchev, M.; Wang, Q. *J. Am. Chem. Soc.* **2006**, *128*, 791–800.

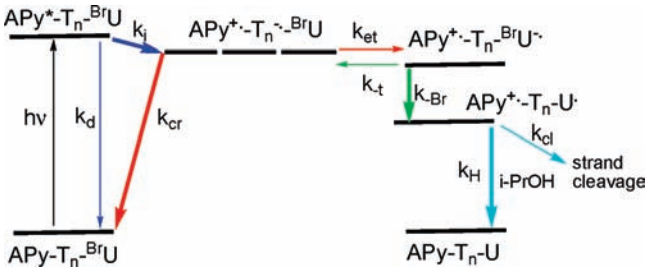

Figure 6. Kinetic scheme for formation of **APy-nU** from **APy-n^{X}U**. Bold arrows show major pathway at the four branching points that determine the overall quantum yield as defined in eq 2.

eq 1. Similar transient spectra and efficient fluorescence quenching are observed for the **APy-n^{Br}U** conjugates.

A kinetic scheme for photoinduced charge separation, charge recombination, and product formation is shown in Figure 6. According to this scheme, exergonic electron injection is much faster than radiative or nonradiative decay of APy ^{1}S* ($k_i > k_d$). Ultrafast electron injection was previously observed in our laboratories for singlet stilbenediether-linked DNA hairpins having neighboring A-T or G-C base pairs[23] and duplexes possessing a pyrenyluridine electron donor and a ^{Br}U acceptor[24] but has not been directly observed by transient spectroscopy for other electron donors with pyrimidine acceptors. Similar fast electron injection presumably occurs with other strong electron donors including the diaminonaphthalene and diaminostilbene derivatives employed by Rokita and Ito in their studies of DNA electron transport.[9−11]

The decay of the transient spectra of the APy conjugates (Figures 2b, 3) is best fit as a dual exponential (Table 1) having a major shorter-lived component (2.4−7.1 ps, 87−96%) and minor longer-lived component (43−66 ps, 4−13%). Both components are assigned to APy$^{+\bullet}$ charge recombination on the basis of their similar time-resolved spectra (Figure S5, Supporting Information). Dual exponential decay may reflect the presence of two kinetically nonequivalent conformations for the APy conjugates. Somewhat slower multiple exponential decay has been observed for duplexes possessing a pyrenyluridine electron donor and a ^{Br}U acceptor.[24] The dispersion of lifetimes was attributed to multiple conformations. DNA duplexes possessing 5′- or 3′-tethered pyrene derivatives have been suggested to adopt both intercalated and end-capped conformations.[52] The transient spectra of the APy conjugates decay completely in <1 ns, leaving no residual long-lived APy$^{+\bullet}$ transients (Figures 2b, 3). The absence of long-lived transients indicates that the APy$^{+\bullet}$-T$^{-\bullet}$ and APy$^{+\bullet}$-^{Br}U$^{-\bullet}$ charge-separated states decay predominately via charge recombination (k_{cr}, Figure 6).

The decay times of major short-lived transient components increase slightly as the separation between APy and ^{Br}U increases (Table 1). However, these decay times are much shorter and their distance dependence is much smaller than would be expected for APy$^{+\bullet}$-T$_n$-^{Br}U$^{-\bullet}$ charge recombination via a single step tunneling processes.[53,54] The small variation in decay times suggests that charge recombination occurs predominantly from the contact radical ion pair in all cases (Figure 6, k_{cr}). The weak distance dependence may reflect the influence of the stable ^{Br}U-A base pair at various locations upon the base pair conformational mobility.

Photochemical Behavior of the APy-n^{X}U Conjugates. Formation of **APy-nU** conjugates upon irradiation of **APy-n^{X}U** plausibly occurs via loss of halide ions from the APy$^{+\bullet}$-T$_n$-^{Br}U$^{-\bullet}$ charge-separated state followed by scavenging of the uracilyl radical by *i*-PrOH (Figure 6, k_{-Br} and k_H). Loss of bromide from ^{Br}U$^{-\bullet}$ has been studied under a variety of conditions including attachment of solvated electrons generated by pulse radiolysis to ^{Br}U,[20,21] direct irradiation of ^{Br}U-containing oligonucleotides,[41,55] and photoreduction of oligonucleotide conjugates containing ^{Br}U.[12,13] Loss of bromide and iodide from reduced ^{Br}U and ^{I}U in the gas phase is estimated to be exergonic by 0.24 and 0.42 eV, respectively. A nanosecond pulse radiolysis study provides half-lives of 7 and 1.7 ns for loss of bromide and iodide, respectively, from the reduced bases in water,[56] consistent with the small calculated barriers for loss of halide ions.[28]

In the absence of added free radical scavengers, the uracilyl radical abstracts a hydrogen atom from the C1′ or C2′ position of the 5′-nucleotide, resulting in the formation of a base-labile lesion.[41] However, the uracilyl radical can be scavenged by 100 mM *i*-PrOH, resulting in formation of the corresponding intact U-containing oligonucleotide.[57] The good mass balance observed in our HPLC analyses (Figure S7, Supporting Information) indicates that uracilyl radical scavenging is highly efficient (Figure 6, $k_H > k_{cl}$). Mannetto et al. recently reported scavenging by EDTA of the uracilyl radical formed upon irradiation of reduced flavin-linked hairpins containing ^{Br}U, permitting analysis of the intact hairpins by capillary electrophoresis. This technique provides excellent resolution of reactant and product peaks.[12] Our plots of conversion vs irradiation time (Figure 4) are similar to those reported by these workers.

According to the simplified kinetic scheme shown in Figure 6 product formation from the BrU conjugates requires four sequential steps (a) electron injection to T$_n$ (k_i), (b) electron transport to ^{Br}U (k_{et}), loss of bromide (k_{-Br}), and scavenging of the uracilyl radical by *i*-PrOH (k_H). Based on this scheme, the quantum yield Φ_U is defined in eq 2 as the product of the probabilities for each of these steps.

$$\Phi_U = \Phi_{cs}\cdot\Phi_{et}\cdot\Phi_{-X}\cdot\Phi_H = k_i(k_i + k_d)\cdot k_{et}/(k_{et} + k_{cr})\cdot k_{-X}(k_{-X} + k_{-t})\cdot(k_H/k_H + k_{cl}) \quad (2)$$

As previously discussed, efficient fluorescence quenching and ultrafast formation of the APy$^{+\bullet}$ transient absorption band indicate that $\Phi_{cs} \approx 1.0$ ($k_{cs} \gg k_d$) and the good mass balance for conversion of reactants to products indicates that $\Phi_H \approx 1.0$ ($k_H \gg k_{cl}$). This leaves charge transport (Φ_{et}) and loss of halide ions (Φ_{-X}) as the possible sources of inefficiency. The reported rate constants for loss of halide from ^{Br}U and ^{I}U (1.4 and 5.9 × 10^8 s^{-1}, respectively[56]) are faster than single step charge recombination across several base pairs.[15] Furthermore, values of Φ_U are similar for **APy-n^{Br}U** and **APy-n^{I}U** when $n = 3$ or 4 (Figure 6) even though loss of I$^-$ is faster than loss of Br$^-$. Thus it is unlikely that thermal detrapping (k_{-t}, Figure 6) competes with loss of halide ions. The ability of ^{Br}U and ^{I}U to serve as effective electron traps is consistent with our measured

(52) (a) Mann, J. S.; Shibata, Y.; Meehan, T. *Bioconjugate Chem.* **1992**, *3*, 554–558. (b) Printz, M.; Richert, C. *Chem.—Eur. J.* **2009**, *15*, 3390–3402.
(53) Jortner, J.; Bixon, M.; Langenbacher, T.; Michel-Beyerle, M. E. *Proc. Natl. Acad. Sci. U.S.A.* **1998**, *95*, 12759–12765.
(54) Blaustein, G. S.; Dernas, B.; Lewis, F. D.; Burin, A. L. *J. Am. Chem. Soc.* **2009**, *131*, 400–401.
(55) Chen, T.; Cook, G. P.; Koppisch, A. T.; Greenberg, M. M. *J. Am. Chem. Soc.* **2000**, *122*, 3861–3866.
(56) Rivera, E.; Schuler, R. H. *J. Phys. Chem.* **1983**, *87*, 3966–3971.
(57) Sugiyama, H.; Fujimoto, K.; Saito, I. *Tetrahedron Lett.* **1997**, *38*, 8057–8060.

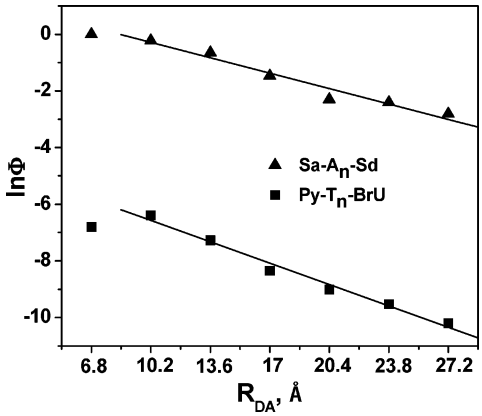

Figure 7. Distance dependence of the quantum yields for formation of **APy-nU** from **APy-n^{Br}U** (■) and for hole transport in **Sa-A$_n$-Sd** capped hairpins having a stilbenedicarboxamide acceptor and stilbene diether donor separated by polyA-polyT base pair domains (▲, data from ref 16). Distances (R_{DA}) are calculated assuming an average π-stacking distance of 3.4 Å for B-DNA hairpins.[61]

reduction potentials for ^{Br}U or ^{I}U vs T as well as a recent report by Ito et al. that loss of bromide from a duplex having a phenothiazine donor and two ^{Br}U bases separated by a single cytosine occurs only at the ^{Br}U site proximate to the donor.[58]

On the basis of the above process of elimination, the low values of Φ_U can be attributed to inefficient electron transport from the APy$^{+\bullet}$-T$^{-\bullet}$ charge-separated state to ^{Br}U ($k_{et} \ll k_{cr}$, Figure 6). The major transient decay component for the APy$^{+\bullet}$-T$^{-\bullet}$ charge-separated state provides a value of $k_{cr} = 2 \times 10^{11}$ s^{-1}, substantially faster than the value of $k_{et} \approx 1 \times 10^9$ s^{-1} we have determined for hole transport across a single A-T base pair.[59] Assuming that the value of k_{et} for electron transport is comparable to or slower than that for hole transport, as suggested by a report for another DNA-based system,[21] we conclude that *fast radical ion pair charge recombination is the major source of inefficiency in the formation of dehalogenated products*.

The lower values of Φ_U for **APy-2^{X}U** vs **APy-3^{X}U** conjugates (Figure 5) plausibly reflect faster charge recombination from the APy$^{+\bullet}$-T$_n$^{Br}U$^{-\bullet}$ charge-separated state via a single step tunneling mechanism (this process is omitted for clarity in Figure 6).[15] Values of Φ_U for the **APy-n^{Br}U** conjugates having $n \geq 3$ decrease by a factor of 2 for each additional A-T base pair (Figure 5), suggestive of either a random walk or polaron drift mechanism for electron transport.[53,60] A plot of ln(Φ_U) vs n is shown in Figure 7. A least-squares fit to the data for $n \geq 3$ provides a value for the distance dependence of product formation ($\ln\Phi_U = Ae^{-\beta R}$) of $\beta = 0.22 \pm 0.015$ Å^{-1}. The linear nature of this plot suggests that the distance dependence of Φ_U is determined by a single kinetic parameter, most likely the rate constant for hole transport, k_{et} (Figure 6). Only in such cases can relative quantum yields be used as surrogates for dynamics. Our value of β is somewhat larger than values previously reported for the distance dependence of the relative yields for electron transport using Ir(III)-sensitized loss of bromide from ^{Br}U ($\beta = 0.12$ Å^{-1}),[13] flavin-sensitized cleavage of the $T<>T$ dimer ($\beta = 0.11$ Å^{-1}),[5] and flavin-sensitized cleavage of thymine oxetane ($\beta = 0.16$ Å^{-1}).[8] However, given the different electron donors and acceptors and analytical methods used in these studies, the relatively good agreement between their β values indicates that electron transport across a poly(A)-poly(T) base pair domain depends only weakly on the method of investigation.

Also shown in Figure 7 is our data for the distance-dependent quantum yield for charge separation via A-tract hole transport (Φ_{cs}) in capped hairpins having having a stilbenedicarboxamide acceptor and stilbene diether donor separated by polyA-polyT base pair domains of variable length (**Sa-A$_n$-Sd**).[16] Values of Φ_{cs} are much larger in this system than for the **APy-n^{Br}U** hairpins as a consequence of a larger energy gap for charge recombination, which results in slower rate constants for this process. However, the value of $\beta = 0.16 \pm 0.017$ for hole transport in **Sa-A$_n$-Sd** is similar to the values of β for electron transport summarized above. Thus we concur with the recent finding of Barton and co-workers that electron and hole transport in A-tracts display similar weak distance dependence.[13]

Concluding Remarks. The singlet excited state of APy is a strong electron donor capable of rapid and efficient electron injection to an adjacent thymine, resulting in formation of APy$^{+\bullet}$ which can be characterized by its transient absorption spectrum. Unlike pyrene derivatives that have higher oxidation potentials,[24,31] hole injection to purine bases does not compete with electron injection into pyrimidine bases in the case of APy. However, the singlet radical ion pair undergoes rapid charge recombination, resulting in low overall electron transport efficiencies. This is likely to be the case for other strong singlet state electron donors including other aminoarenes and stilbenediether.[9−11]

Following electron injection from singlet APy into the neighboring T, electron transport and trapping by the halouracil derivatives ^{Br}U and ^{I}U results in formation of the APy$^{+\bullet}$-^{X}U$^{-\bullet}$ charge-separated states. The reduced halouracils undergo loss of halide to from uracilyl radicals which are efficiently scavenged by *i*-PrOH to form the intact **APy-nU** conjugates.[57] Conversion of the halouracil conjugates to the corresponding uracil conjugates can be conveniently monitored by HPLC or MALDI-TOF mass spec, providing a simple method for determination of relative and absolute quantum yields. Reductive cleavage of thymine dimers and a thymine oxetane also have been employed as chemical probes for electron transport and have low quantum yields.[4,8]

Our results serve to clarify the origins of some of the seemingly conflicting results obtained in previous studies of DNA electron transport. Reversible electron injection and trapping and slow loss of halide from reduced halouracils can account for the strong distance dependence observed by Kawai and by Fiebig.[21,24] Barton and co-workers avoided these problems by the use of the flash-quench technique to generate a ground state reductant capable of reducing both T and ^{Br}U.[13] Their method provides relative yields of strand cleavage but neither quantum yields nor kinetic data.

Our results also establish that the distance dependence of the relative efficiency of electron transport across polyA:polyT base pair domains parallels that for hole transport in stilbene-capped hairpins.[33,59] However, the quantum yield for hole transport across six A-T base pairs in stilbene-capped hairpins is significantly larger than for loss of bromide following electron transport (0.09 vs 1.2×10^{-4}). Future quantitative studies of the dynamics and efficiency of electron transport in DNA will

(58) Ito, T.; Kondo, A.; Terada, S.; Nishimoto, S. *J. Am. Chem. Soc.* **2006**, *128*, 10934–10942.
(59) Lewis, F. D.; Zhu, H.; Daublain, P.; Cohen, B.; Wasielewski, M. R. *Angew. Chem., Int. Ed.* **2006**, *45*, 7982–7985.
(60) Conwell, E. M.; Rakhmanova, S. V. *Proc. Natl. Acad. Sci. U.S.A.* **2000**, *97*, 4556–4560.
(61) Egli, M.; Tereshko, V.; Mushudov, R.; Sanishvili, R.; Liu, X.; Lewis, F. D. *J. Am. Chem. Soc.* **2003**, *125*, 10842–10849.

require the development of chromophores for electron injection which have slower rate constants for charge recombination than the aminopyrene used in this study and of electron acceptors that have a spectroscopic signature upon electron capture. Such studies are in progress in our laboratory.

Experimental Section

General Procedures. UV absorption, fluorescence, and circular dichroism spectra were obtained as previously described on samples contained in 1 cm path length cuvettes.[15] Quantum yields for fluorescence were determined using quinine sulfate in sulfuric acid as a reference standard.[62] CD spectra are the average of 2 scans with a data interval of 1.0 nm and a time interval of 2 s per point. The base lines are corrected by subtraction of the spectrum of the buffer (10 mM phosphate, 0.1 M NaCl). Electrochemical measurements were performed using a CH Instruments Model 622 electrochemical workstation. The solvent was dimethyl formamide containing 0.1 M tetra-*n*-butylammonium hexafluorophosphate electrolyte. A glassy carbon working electrode, platinum wire counter electrode, and Ag/AgCl reference electrode were employed. Ferrocene/ferrocinium (Fc/Fc^+, 0.47 vs SCE in DMF[46]) was used as an internal reference for all measurements.

All samples for kinetic spectroscopic measurements were prepared in 10 mM sodium phosphate, pH 7.2, buffer with 0.1 M NaCl (standard buffer). Samples were stirred during these measurements and absorption spectra checked before and after spectroscopic studies for the occurrence of decomposition. Hairpin concentrations were adjusted to provide an absorbance of 0.2 at 354 nm in a 1 cm path length cuvette for fluorescence measurements and 0.27 in a 1 mm path length cell for pump−probe measurements. Fluorescence decay measurements, nanosecond transient absorption measurements, and femtosecond broadband pump−probe spectra were obtained as previously described.[15]

Samples of hairpin conjugates for quantitative photochemical studies having an optical density of 0.02 at 390 nm were prepared in standard buffer containing 0.1 M isopropyl alcohol (*i*-PrOH). Samples (1.7 mL) were placed in quartz cuvettes equipped with a stirring bar and a rubber septum and were purged with dry nitrogen for 15 min prior to irradiation. Samples were irradiated in a thermostatted cuvette holder at 20 °C with monochromatic 390 nm light provided by a 150 W mercury arc lamp and a 0.5 M monochromator. For HPLC analysis 5.0 μL aliquots were withdrawn by syringe at regular time intervals and analyzed by HPLC using a Varian Microsorb-MV100 C18 column on a Dionex HPLC system equipped with a diode array detector. Solutions of (A) 0.03 M TEAA and (B) 95% acetonitrile and 5% 0.03 M TEAA were used as the mobile phase. A gradient of 5 min 0−16% B, followed by an isocratic elution (16% B-84% A) with a flow rate of 1 mL/min was use for the separation. Integration of HPLC peaks using detection wavelengths of 260 nm (base pair) and 350 nm (pyrene) provided similar results. For MALDI analysis the overlapping reactant and product peaks were collected by HPLC, the solvent evaporated and the residue dissolved in 10 μL water. Half of this solution was used to prepare 5 spots on the MALDI plate. Integrated HPLC or MALDI peak areas were used to construct plots of % conversion vs irradiation time (Figures 4 and S8, Supporting Information). Relative quantum yields were determined from the initial slopes of these plots. Absolute quantum yields for **APy-4^{Br}U** were determined at low conversions (<25%) of reactant to product (average of three independent HPLC analyses) using potassium ferrioxalate actinometry[45] to determine the intensity of absorbed light. The resulting quantum yield was used to convert the relative quantum yields to absolute quantum yields.

Materials

***N*-(3-Hydroxybutyl)-1-aminopyrene (APy-H).** Reaction of 1-aminopyrene with butyrolactone in the presence of dimethylaluminumchloride following the procedure of Barrett and Dhanak[63] afforded 4-(pyren-1-ylamino)butan-1-ol as a white solid. Reduction with excess lithium aluminum hydride provided APy-H in 85% yield which was further purified by column chromatography, mp 99−101 °C. ^{1}H NMR (500 MHz, DMSO-d_6): δ 8.5 (1H, d), 8.2 (2H, t), 8.0 (5H, m), 7.9 (1H, d), 7.2 (2H, t), 6.7 (3H, m), 6.2 (1H, b), 3.7 (2H, dd), 3.5 (2H, t), 3.0 (3H, s), 2 (2H, t). ^{13}C NMR (DMSO-d_6): δ 143.72, 132.13, 131.56, 127.80, 126.83, 125.97, 125.56, 125.15, 124.37, 122.94, 122.46, 121.86, 121.49, 120.96, 115.36, 108.22, 60.65, 43.13, 30.37, 25.19 ppm. ESI-MS/MS *m*/*z* (% relative intensity): 288.10 [100, $(M-H)^+$], 289.10 [30, M^+].

Hairpin Conjugates. APy-H was converted to its phosphoramidite derivative in 85% yield following the method of Letsinger and Wu.[64] This derivative was attached to the 5′-terminus of an oligonucleotide which was prepared using conventional solid-supported phosphoramidite synthesis. The conjugates were deprotected using 30% ammonium hydroxide and purified by RP HPLC. Structures confirmed by MALDI-TOF-MS (Table S1, Supporting Information).

Acknowledgment. This research is supported by grants from the Chemical Sciences, Geosciences and Biosciences Division, Office of Basic Energy Sciences, Office of Science, U.S. Department of Energy (DE-FG02-96ER14604 to FDL and the National Science Foundation (CHE-0628130 to T.F.).

Supporting Information Available: MALDI-TOF analysis for capped hairpins, ZINDO-derived UV spectra, UV, fluorescence, and circular dichroism spectra, thermal dissociation profiles, species-associated transient absorption spectra, HPLC data for irradiated solutions, and plots of conversion vs irradiation time for the iodouracil conjugates. This material is available free of charge via the Internet at http://pubs.acs.org.

JA905140N

(62) Berlman, I. B. *Handbook of Fluorescence Spectra of Aromatic Molecules*, 2nd ed.; Academic Press: New York, 1971.
(63) Barrett, A. G. M.; Dhanak, D. *Tetrahedron Lett.* **1987**, *28*, 3327–3330.
(64) Letsinger, R. L.; Wu, T. *J. Am. Chem. Soc.* **1995**, *117*, 7323–7328.